THEORETICAL & APPLIED MECHANICS LETTERS **2**, 013001 (2012)

Multi-modes control method for spacecraft formation establishment and reconfiguration near the libration points

Yuedong Zhang, Yunhe Meng,[a)] and Jinhai Dai
College of Aerospace and Material Engineering, National University of Defense Technology, Changsha 410073, China

(Received 24 July 2011; accepted 26 September 2011; published online 10 January 2012)

Abstract This paper studies Multi-modes control method for libration points formation establishment and reconfiguration. Firstly, relations between optimal impulse control and Floquet modes are investigated. Method of generating modes is proposed. Characteristics of the mode coefficients stimulated at different time are also given. Studies show that coefficients of controlled modes can be classified into four types, and formation establishment and reconfiguration can be achieved by multi-impulse control with the presented method of generating modes. Then, since libration points formation is generally unstable, mutli-modes keeping control method which can stabilize five Floquet modes simultaneously is proposed. Finally, simulation on formation establishment and reconfiguration are carried out by using method of generating modes and mutli-modes keeping control method. Results show that the proposed control method is effective and practical. [doi:10.1063/2.1201301]

Keywords circular restricted three-body problem, libration points, spacecraft formation flying, floquet modes, formation establishment and reconfiguration

Libration point orbits (LPOs), a subset of periodic orbits in circular restricted three-body problem (CRTBP),[1] have enjoyed a growing prominence in mission design. Over the last 30 years, several more missions have flown on these three-body trajectories, and many are still in orbit collecting data, including ACE, SOHO, WMAP, ARTEMIS.[2,3] At present, interest in LPOs continues to increase and mainly focuses on the relative motion problem of LPOs, such as deployment of spacecraft formation in LPOs to achieve long baseline interferometry,[4] and research on rendezvous and docking between the satellites and the space stations in LPOs.[5]

Compared with two-body problem, the relative motion problem of the LPOs is more complicated due to its nonlinear characteristic. Extensive progress in the relative motion problem of LPOs has been achieved. Richardson obtained the third-order expansions of the nonlinear relative motion.[6] Howell and Barden investigated formation flying in the vicinity of the libration points in the circular restricted three-body problem. Initially, their focus was the determination of the natural behavior on the center manifold near the libration points.[7] In a later work, the control strategies were shown to be effective in the full ephemeris model, include input-state feedback linearization and output-state feedback linearization, linear quadratic regulator theory, and impulsive maneuvers derived via a differential corrections scheme.[8,9] Gurfil et al. studied the invariant manifolds of relative motion and provided a measurement method.[10] Gong et al. studied two-impulse maneuver method for formation in LPOs, the beginning-ending method was proven to be an energy-optimal one of all two-impulse reconfigurations.[11,12] Peng et al.[13] proposed an optimal periodic controller for spacecraft formation in LPOs. A new numerical algorithm for solving the periodic Riccati differential equation is proposed based on the geometric structure of Hamiltonian system.[13] Characteristic exponent assignment method and adaptive neural control method was also studied for stabilizing the relative motion of LPOs.[14,15]

Gómez et al. proposed the Floquet modes of LPOs and the method of calculation.[16,17] With the Floquet modes, relative motion state of the LPOs can be expressed as a linear combination of six Floquet modes, which are the divergence mode, the convergence mode, and four periodic modes. Consequently, there is an inner link between the Floquet periodic modes and the relative motion of LPOs. Station-keeping control methods for LPOs based on Floquet theory have been also studied by Gómez et al.,[16] Simó et al.[18] and Howell et al.[19] Lü et al.[20] proposed a continuous thrust control strategy to eradicate the dominant unstable component of LPOs. Using transformed coordinate system the linear part of dynamical equations can be expressed in a standard form. The advantage of proposed method is of no need to determine a nominal orbit as a reference path.[20]

In former work, we have shown that configuration of libration points spacecraft formation can be designed by using four periodic Floquet modes, and several special formation configurations have been obtained.[21]

In this paper, problem of libration points formation establishment and reconfiguration is studied. Firstly, dynamic model of the circular restricted three body problem is introduced. Secondly, the modes generating method using optimal Floquet control strategy is investigated. Then, muti-modes control method which

a) Corresponding author. Email: myh_world@163.com.

can stabilize five Floquet modes simultaneously is proposed. Finally, simulation on formation establishment and reconfiguration is carried out.

Given two point masses m_1 and m_2, the circular restricted three body problem (CRTBP) studies the motion of a third point mass m_3, whose dynamics is affected by, but does not affect, m_1 and m_2, which are called the primaries. The primaries move along a circular orbit. After normalization in the synodic reference frame, the equations of motion for m_3 in the CRTBP are of the form[8]

$$\begin{aligned} \ddot{x} - 2\dot{y} &= \frac{\partial \Omega}{\partial x}, \\ \ddot{y} + 2\dot{x} &= \frac{\partial \Omega}{\partial y}, \\ \ddot{z} &= \frac{\partial \Omega}{\partial z}, \end{aligned} \tag{1}$$

with

$$\Omega(x, y, \mu) = \frac{1}{2}(x^2 + y^2) + \frac{1-\mu}{r_1} + \frac{\mu}{r_2} + \frac{\mu(1-\mu)}{2},$$

where

$$\mu = m_1/(m_1 + m_2),$$

r_1 and r_2 denote the distances of m_1 and m_2 from the center of mass of the system

$$\begin{aligned} r_1 &= \left[(x+\mu)^2 + y^2 + z^2\right]^{1/2}, \\ r_2 &= \left[(x+\mu-1)^2 + y^2 + z^2\right]^{1/2}. \end{aligned}$$

Let $\tilde{X}$ represent a reference LPOs, then $\delta \boldsymbol{X} = \boldsymbol{X} - \tilde{\boldsymbol{X}}$ represents the variation with respect to it. The linear variational equation of motion in the CRTBP can be derived in matrix form as

$$\delta \dot{\boldsymbol{X}} = \boldsymbol{A}(t) \cdot \delta \boldsymbol{X}. \tag{2}$$

$\boldsymbol{A}(t)$ is periodic and time-varying, which has the form

$$\boldsymbol{A}(t) = \begin{bmatrix} 0 & 0 & 0 & 1 & 0 & 0 \\ 0 & 0 & 0 & 0 & 1 & 0 \\ 0 & 0 & 0 & 0 & 0 & 1 \\ \Omega_{xx} & \Omega_{xy} & \Omega_{xz} & 0 & 2 & 0 \\ \Omega_{yx} & \Omega_{yy} & \Omega_{yz} & -2 & 0 & 0 \\ \Omega_{zx} & \Omega_{zy} & \Omega_{zz} & 0 & 0 & 0 \end{bmatrix}. \tag{3}$$

Formation establishment and reconfiguration can be achieved via two stages. First stage is the modes generation. Modes combination of desired configuration will be generated based on optimal Floquet control strategy. Second stage is to keep the newly formed configuration. Five Floquet modes will be stabilized simultaneously at this stage.

Gómez et al.[16] proposed the optimal impulse control strategy for eliminating mode 4 in the study of the transfer between Halo orbits

$$\boldsymbol{e}_4(\tau) + \begin{pmatrix} \boldsymbol{0}_{3\times 1} \\ \Delta \boldsymbol{v}_{3\times 1} \end{pmatrix} = \alpha_2 \boldsymbol{e}_2(\tau) + \alpha_3 \boldsymbol{e}_3(\tau) +$$

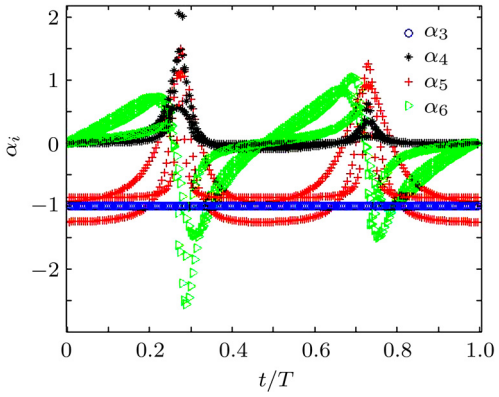

Fig. 1. The modes coefficients stimulated by impulse control form Eq. (4).

$$\alpha_4 \boldsymbol{e}_4(\tau) + \alpha_5 \boldsymbol{e}_5(\tau) + \alpha_6 \boldsymbol{e}_6(\tau), \tag{4}$$

with Eq. (4), mode $\boldsymbol{e}_4$ can be expressed by other modes (mode 2, 3, 5, 6). There are seven unknown variables ($\Delta \boldsymbol{v}_{3\times 1}$, α_2, α_3, α_5, α_6) in six-dimensional equations, so adding some optimal condition such as $|\Delta \boldsymbol{v}_{3\times 1}|$ to be a minimum, we can compute the value of $\Delta \boldsymbol{v}_{3\times 1}$.

Similarly, we get the optimal impulse control strategy for eliminating other modes. The equations are

$$\boldsymbol{e}_6(\tau) + \begin{pmatrix} \boldsymbol{0}_{3\times 1} \\ \Delta \boldsymbol{v}_{3\times 1} \end{pmatrix} = \alpha_2 \boldsymbol{e}_2(\tau) + \alpha_3 \boldsymbol{e}_3(\tau) + \alpha_4 \boldsymbol{e}_4(\tau) + \alpha_5 \boldsymbol{e}_5(\tau), \tag{5}$$

$$\boldsymbol{e}_3(\tau) + \begin{pmatrix} \boldsymbol{0}_{3\times 1} \\ \Delta \boldsymbol{v}_{3\times 1} \end{pmatrix} = \alpha_2 \boldsymbol{e}_2(\tau) + \alpha_4 \boldsymbol{e}_4(\tau) + \alpha_5 \boldsymbol{e}_5(\tau) + \alpha_6 \boldsymbol{e}_6(\tau), \tag{6}$$

$$\boldsymbol{e}_5(\tau) + \begin{pmatrix} \boldsymbol{0}_{3\times 1} \\ \Delta \boldsymbol{v}_{3\times 1} \end{pmatrix} = \alpha_2 \boldsymbol{e}_2(\tau) + \alpha_3 \boldsymbol{e}_3(\tau) + \alpha_4 \boldsymbol{e}_4(\tau) + \alpha_6 \boldsymbol{e}_6(\tau). \tag{7}$$

To make a forward study on the relations between the optimal impulse control and Floquet modes, following simulations are carried out. Parameters of three specific Halo orbits are listed in Table 1, where $\tilde{X}_0$ and T represent initial values and periods of reference Halo orbits in normalized units, respectively.

Supposing that the initial states of the surrounding spacecraft is the same as the reference spacecraft, we impose four kinds of optimal Floquet control strategies. The periodic modes coefficients curves are shown in Figs. 1–4. Each mode is represented by different symbolic and three curves correspond to three reference Halo orbits.

From Figs. 1–4, the following conclusions can be summarized:

(1) The optimal control strategy can produce a stable mode and will also cause changes of other three modes.

Table 1. The parameters of three reference Halo orbits

	$\tilde{X} = \left[\begin{array}{cccccc} x & y & z & \dot{x} & \dot{y} & \dot{z} \end{array}\right]$	T
Orbit 1	[0.823 368 92 0 0.004 072 73 0 0.126 614 79 0]	2.743 072 12
Orbit 2	[0.823 363 25 0 0.010 408 08 0 0.128 124 16 0]	2.743 699 52
Orbit 3	[0.823 365 17 0 0.022 400 00 0 0.134 278 08 0]	2.746 337 69

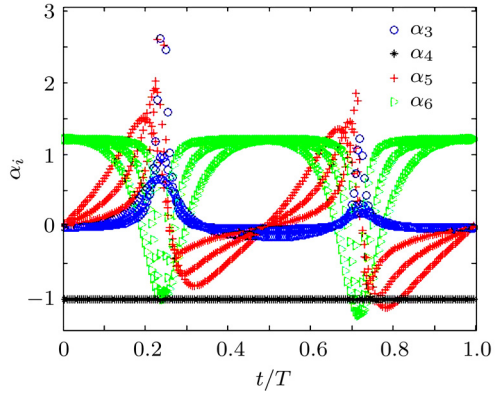

Fig. 2. The modes coefficients stimulated by impulse control form Eq. (5).

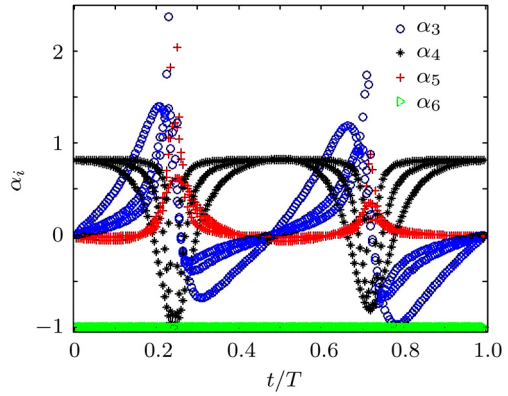

Fig. 4. The modes coefficients stimulated by impulse control form Eq. (7).

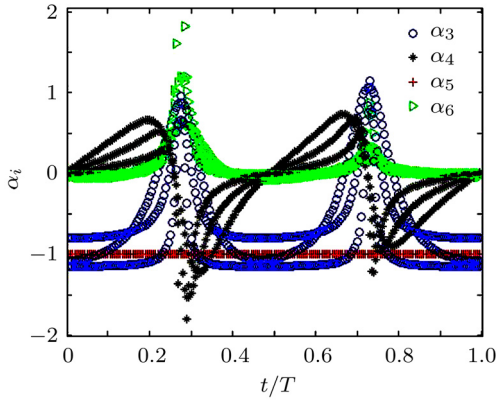

Fig. 3. The modes coefficients stimulated by impulse control form Eq. (6).

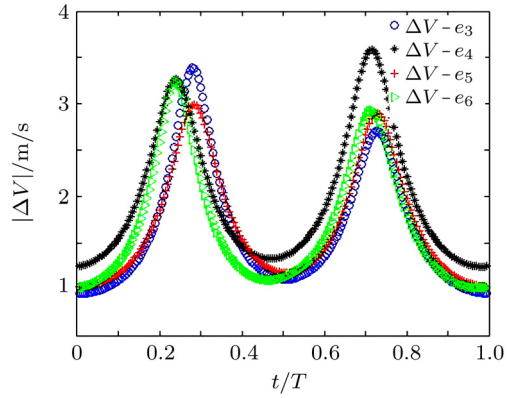

Fig. 5. The curve of impulse control energy along with time instant.

(2) The coefficients of controlled modes are classified into four types:

(a) "Constant type", which corresponds to the curve of α_3 in Fig. 1.

(b) "Bimodal type with the zero start and zero end", which corresponds to curve of α_4 in Fig. 1.

(c) "Bimodal type with the non-zero start and non-zero end", which corresponds to curve of α_5 in Fig. 1.

(d) "Bimodal and double valley type", which corresponds to curve of α_6 in Fig. 1.

Other modal types stimulated by optimal impulse control are listed in Table 2.

(3) With the decrease of z-amplitude of Halo orbit, the peak values of mode coefficient curves become sharp. To the opposite, if the z-amplitude of Halo orbit increases, the peak values of mode coefficient curves will become smooth.

(4) The optimal impulse control will always generate modes $\boldsymbol{e}_3$, $\boldsymbol{e}_5$ (or $\boldsymbol{e}_4$, $\boldsymbol{e}_6$) in pairs. If the optimal impulse is applied near the peak of the "Non-zero bimodal type ", the modes $\boldsymbol{e}_3$, $\boldsymbol{e}_5$ (or $\boldsymbol{e}_4$, $\boldsymbol{e}_6$) will be generated with opposite signs.

Further studies show that modes imposed by the impulse control are different but the trends are almost the same for four kind of modes within T. As shown in Fig. 5, the minimum control energies are at $t = 0\ T$ and $t = 0.5\ T$ while the maximum control energies cost

Table 2. Modal types stimulated by optimal impulse control.

	Controlled modes	Constant type	Zero bimodal type	Non-zero bimodal type	Bimodal and double valley type
Fig. 1	$\boldsymbol{e}_3$	$\boldsymbol{e}_3$	$\boldsymbol{e}_4$	$\boldsymbol{e}_5$	$\boldsymbol{e}_6$
Fig. 2	$\boldsymbol{e}_4$	$\boldsymbol{e}_4$	$\boldsymbol{e}_3$	$\boldsymbol{e}_6$	$\boldsymbol{e}_5$
Fig. 3	$\boldsymbol{e}_5$	$\boldsymbol{e}_5$	$\boldsymbol{e}_6$	$\boldsymbol{e}_3$	$\boldsymbol{e}_4$
Fig. 4	$\boldsymbol{e}_6$	$\boldsymbol{e}_6$	$\boldsymbol{e}_5$	$\boldsymbol{e}_4$	$\boldsymbol{e}_3$

are at $t = 0.3\ T$ and $t = 0.7\ T$. So the appropriate control time can be selected in the vicinity of $0.3\ T$ and $0.7\ T$. These results indicate that proper time of control operation should be considered.

Howell et al.[19] proposed two types of strategies for controlling three Floquet modes simultaneously, however, it is not fit for formation establishment and reconfiguration because five Floquet modes should be controlled simultaneously. In the problem of formation establishment and reconfiguration, unstable mode $\delta\boldsymbol{X}_1$, needs to be totally or substantially eliminated. The stable mode 2 needs not to be controlled. Four periodic modes should be stably controlled at the designed value. That is to say, except the stable mode, five Floquet modes must be controlled simultaneously.

The initial state deviation can be expressed as

$$\Delta\delta\boldsymbol{X}_c = \delta\boldsymbol{X}_1(t) + \Delta\delta\boldsymbol{X}_3(t) + \Delta\delta\boldsymbol{X}_4(t) + \Delta\delta\boldsymbol{X}_5(t) + \Delta\delta\boldsymbol{X}_6(t) \tag{8}$$

where

$$\Delta\delta\boldsymbol{X}_j(t) = \delta\boldsymbol{X}_j(t) - \delta\tilde{\boldsymbol{X}}_j(t) = [c_j(t) - \tilde{c}_j(t)]\,\boldsymbol{e}_j(t), \quad j = 3,4,5,6.$$

Studies show that it is impossible to eliminate all of $\delta\boldsymbol{X}_c$ in one impulse,[4] thus to make the state deviation converge continuously, the gradual control manner should be adopted

$$\Delta\delta\boldsymbol{X}_c + \begin{bmatrix} \boldsymbol{0}_{3\times1} \\ \Delta\boldsymbol{V}_{3\times1} \end{bmatrix} = \alpha_3\cdot\boldsymbol{e}_3(t) + \alpha_4\cdot\boldsymbol{e}_4(t) + \alpha_5\cdot\boldsymbol{e}_5(t) + \alpha_6\cdot\boldsymbol{e}_6(t) + \alpha_2\cdot\boldsymbol{e}_2(t), \tag{9}$$

where the expression of

$$\left|\frac{\alpha_j}{c_j(t) - \tilde{c}_j(t)}\right| < 1\ , \quad j = 3,4,5,6$$

should be satisfied to diminish the control error.

After each control, the unstable item will be eliminated and the deviation of coefficients of periodic modes 3–6 will be smaller and smaller which ensures the stability of the designed configuration.

The equation can be transformed into

$$\Delta\delta\boldsymbol{X}_c - \alpha_2\cdot\boldsymbol{e}_2(t) = \begin{bmatrix} \boldsymbol{e}_3(t) & \boldsymbol{e}_4(t) & \boldsymbol{e}_5(t) & \boldsymbol{e}_6(t) & \boldsymbol{0}_{3\times1} \\ & & & & -\boldsymbol{I}_{3\times3} \end{bmatrix} \begin{bmatrix} \boldsymbol{\alpha}_{3,4,5,6} \\ \Delta\boldsymbol{V}_{3\times1} \end{bmatrix}. \tag{10}$$

Equation (10) is ill-posed and of rank deficiency, which transforms one periodic mode from the right side to the left. Take the mode 3 as an example

$$\Delta\delta\boldsymbol{X}_c - \alpha_2\cdot\boldsymbol{e}_2(t) - \alpha_3\cdot\boldsymbol{e}_3(t) = \begin{bmatrix} \boldsymbol{e}_4(t) & \boldsymbol{e}_5(t) & \boldsymbol{e}_6(t) & \boldsymbol{0}_{3\times1} \\ & & & -\boldsymbol{I}_{3\times3} \end{bmatrix} \begin{bmatrix} \boldsymbol{\alpha}_{4,5,6} \\ \Delta\boldsymbol{V}_{3\times1} \end{bmatrix}, \tag{11}$$

The right side of Eq. (11) is full rank and can be solved. Let $\boldsymbol{H} = \begin{bmatrix} \boldsymbol{e}_4(t) & \boldsymbol{e}_5(t) & \boldsymbol{e}_6(t) & \boldsymbol{0}_{3\times1} \\ & & & -\boldsymbol{I}_{3\times3} \end{bmatrix}$, Eq. (11) leads to

$$\begin{bmatrix} \boldsymbol{\alpha}_{4,5,6} \\ \Delta\boldsymbol{V}_{3\times1} \end{bmatrix} = \boldsymbol{H}^{-1}[\Delta\delta\boldsymbol{X}_c - \alpha_2\cdot\boldsymbol{e}_2(t) - \alpha_3\cdot\boldsymbol{e}_3(t)]. \tag{12}$$

Since $\begin{bmatrix} \bar{\alpha}_{4,5,6} \\ \Delta\boldsymbol{V}_{3\times1} \end{bmatrix}$ is determined by α_2, α_3 in Eq. (12), further optimization can be done.

Define

$$\boldsymbol{A} = \boldsymbol{H}^{-1}\cdot\delta\boldsymbol{X}_c, \quad \boldsymbol{B} = \boldsymbol{H}^{-1}\cdot\boldsymbol{e}_2(t)$$
$$\boldsymbol{C} = \boldsymbol{H}^{-1}\cdot\boldsymbol{e}_3(t), \quad \boldsymbol{Z} = \begin{bmatrix} \boldsymbol{\alpha}_{4,5,6} \\ \Delta\boldsymbol{V}_{3\times1} \end{bmatrix}$$

in Eq. (12),

$$\boldsymbol{Z} = \boldsymbol{A} - \alpha_2\cdot\boldsymbol{B} - \alpha_3\cdot\boldsymbol{C}. \tag{13}$$

To minimize $\|\boldsymbol{Z}\|^2$, there would be

$$\alpha_{2,\mathrm{opt}} = \frac{\boldsymbol{A}^{\mathrm{T}}\boldsymbol{B}}{\boldsymbol{B}^{\mathrm{T}}\boldsymbol{B}} - \alpha_{3,\mathrm{opt}}\frac{\boldsymbol{C}^{\mathrm{T}}\boldsymbol{B}}{\boldsymbol{B}^{\mathrm{T}}\boldsymbol{B}},$$
$$\alpha_{3,\mathrm{opt}} = \frac{\left(\boldsymbol{A} - \dfrac{\boldsymbol{A}^{\mathrm{T}}\boldsymbol{B}}{\boldsymbol{B}^{\mathrm{T}}\boldsymbol{B}}\boldsymbol{B}\right)^{\mathrm{T}}\cdot\left(\boldsymbol{C} - \dfrac{\boldsymbol{C}^{\mathrm{T}}\boldsymbol{B}}{\boldsymbol{B}^{\mathrm{T}}\boldsymbol{B}}\boldsymbol{B}\right)^{\mathrm{T}}}{\left(\boldsymbol{C} - \dfrac{\boldsymbol{C}^{\mathrm{T}}\boldsymbol{B}}{\boldsymbol{B}^{\mathrm{T}}\boldsymbol{B}}\boldsymbol{B}\right)^{\mathrm{T}}\cdot\left(\boldsymbol{C} - \dfrac{\boldsymbol{C}^{\mathrm{T}}\boldsymbol{B}}{\boldsymbol{B}^{\mathrm{T}}\boldsymbol{B}}\boldsymbol{B}\right)}. \tag{14}$$

If minimize $\|\boldsymbol{Z}(1:3)\|^2$, we can calculate $\alpha_{2,\mathrm{opt}}$, $\alpha_{3,\mathrm{opt}}$ only by the first three-dimensional matrix of $\boldsymbol{B}, \boldsymbol{C}$.

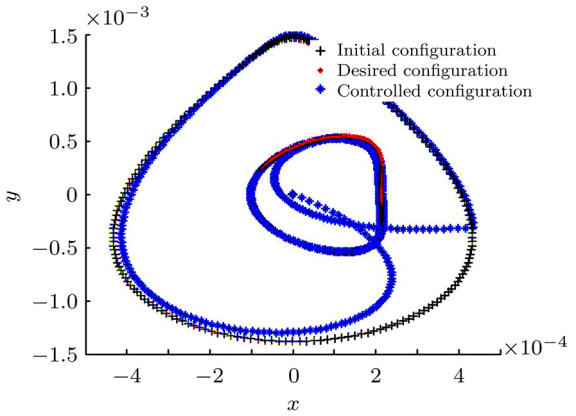

Fig. 6. Formation reconfiguration process.

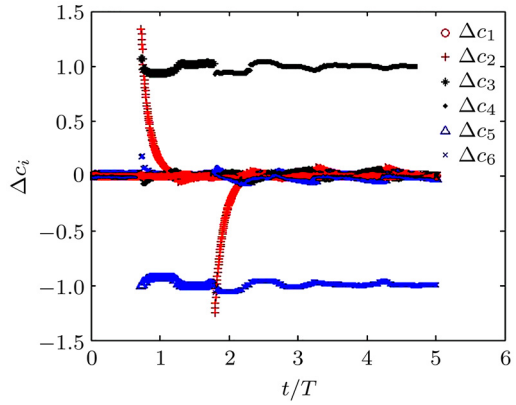

Fig. 7. Modes change during formation reconfiguration.

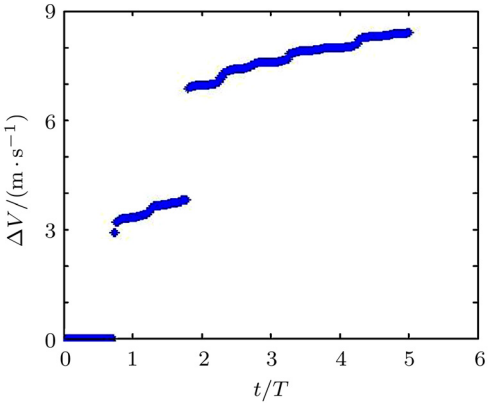

Fig. 8. Fuel consumptions during formation reconfiguration.

There is no constraint on $\alpha_3 \cdot \boldsymbol{e}_3(t)$ and α_3 may increase during formation control. It means that although the control error of the modes $\boldsymbol{\alpha}_{4,5,6}$ converge, the error of the mode 3 may increase. The algorithm can be improved as follows:

(1) Adding a criterion. That is when $|\alpha_{3,\mathrm{opt}}| > 1$, let $\alpha_{3,\mathrm{opt}} = 1$. Since the condition of $|\alpha_{3,\mathrm{opt}}| < 1$ will certainly happen and the error of mode 3 will undoubtedly converge.

(2) Average two corresponding Floquet modes. For example, using

$$\boldsymbol{Z} = \boldsymbol{A} - \alpha_2 \cdot \boldsymbol{B} - \alpha_3 \cdot \boldsymbol{C},$$
$$\boldsymbol{Z} = \boldsymbol{A} - \alpha_2 \cdot \boldsymbol{B} - \alpha_5 \cdot \boldsymbol{C},$$

or

$$\boldsymbol{Z} = \boldsymbol{A} - \alpha_2 \cdot \boldsymbol{B} - \alpha_4 \cdot \boldsymbol{C},$$
$$\boldsymbol{Z} = \boldsymbol{A} - \alpha_2 \cdot \boldsymbol{B} - \alpha_6 \cdot \boldsymbol{C},$$

we can improve the control accuracy.

(3) Average four corresponding Floquet modes. In this way, the control accuracy can be improved further.

Formation reconfiguration process is designed as changing the coefficient from $(\alpha_3 = 0.001, \alpha_5 = -0.001)$ to $(\alpha_4 = 0.001, \alpha_6 = -0.001)$. At $t = 0.72\ T$, modes combination of $\alpha_3 = 0.001$ and $\alpha_5 = -0.001$ is generated by establishment control. At $t = 1.785\ T$, impulse control is imposed to eliminate the mode 3 and mode 5. And modes combination of $\alpha_4 = 0.001$ and $\alpha_6 = -0.001$ is generated at the same time. At last, the maintenance control for mode 4 and mode 6 is carried out. The whole process is shown in Fig. 6, including formation establishment, formation reconfiguration and formation maintenance. Every stage is achieved with high accuracy.

Modes change during formation reconfiguration is shown in Fig. 7. During the process of modes transformation, large stable manifold was created and then decreased exponentially. The mutations of fuel consumptions occur when the impulse control is applied in Fig. 8. Within five orbital period's time about 60 d, hundreds of kilometers of large configuration have been generated and formation reconfiguration have been done with fuel consumption of about 9 m/s. The control frequency is approximately once per day. Values of each impulse is small, so it can be implemented by small thruster or electric thruster.

Deep research on the relations between Floquet modes and impulse control has been done. The modes generating method is studied by using optimal Floquet control strategy. The control method which can stabilize five Floquet modes simultaneously is proposed for formation establishment and reconfiguration. The effectiveness and practicability of the proposed control strategy are testified by simulation.

This work was supported by the National Natural Science Foundation of China (10702078) and the Advance Research Program of National University of Defense Technology (JC08-01-05).

1. E. Kathryn, R. L. Davis, and D. J. Anderson, et al, Celest. Mech. Dyn. Astr. **107**, 471 (2010).
2. D. W. Dunham, and R. W. Farquhar, Libration Point Missions, 1978–2002, in: *Proceedings of the Conference* (World Scientific Publishing Company, Spain, 2003).

3. V. Angelopoulos, Space Science Reviews **141**, 5 (2008).
4. L. D. Millard, and K. C. Howell, Astronautical Science **56**, 71 (2008).
5. L. J. Brian, and H. B. Robert, AIAA-93-3856-CP, 1403 (1993).
6. D. L. Richardson, and W. A. Mitchell, Third-order analytical solution for relative motion with a circular reference orbit, in: *AAS/AIAA 12nd Space Flight Mechanics Meeting*, San Antonio, 2002.
7. B. T. Barden, and K. C. Howell, The Journal of the Astronautical Sciences **46**, 361 (1998).
8. K. C. Howell, and B. G. Marchand, Control strategies for formation flight in the vicinity of the libration points, in: *AIAA/AAS Space Flight Mechanics Conference*, Ponce, Puerto Rico, 2003.
9. B. G. Marchand, and K. C. Howell, Formation flight near L1 and L2 in the Sun–Earth/Moon ephemeris system including solar radiation pressure, in: AAS/AIAA Astrodynamics Specialist Conference, Big Sky, Montana, 2003.
10. P. Gurfil, and K. Kholshevnikov, Annals of the New York Academy of Sciences **1065**, 77 (2005).
11. S. P. Gong, J. F. Li, and H. X. Baoyin, et al., Acta Mechanica Sinica **23**, 321 (2007).
12. S. P. Gong, H. X. Baoyin, and J. F. Li, Transactions of the Japan Society for Aeronautical and Space Sciences **51**, 213 (2009).
13. H. J. Peng, J. Zhao, and Z. G. Wu, et al., Acta Astronautica **69**, 537 (2011).
14. J. Wei, and S. J. Xu, Acta Mechanica Sinica **26**, 495 (2010).
15. P. Li, P. Y. Cui, and H. T. Cui, Acta Mechanica Sinica **25**, 847 (2009).
16. G. Gómez, J. Masdemont, and C. Simó, Acta Astronautica **43**, 493 (1998).
17. G. Gómez, J. Llibre, and R. Martínez, et al., *Dynamics and Mission Design Near Libration Point Orbits (Volume I) Fundamentals: The Case of Collinear Libration Points* (World Scientific Publishing Company, Spain, 2001).
18. C. Simo, G. Gomez, and J. Llibre, et al., Acta Astronautica **15**, 391 (1987).
19. K. C. Howell, and L. D. Millard, Acta Astronautica **64**, 554 (2009).
20. J. Lü, Q. S. Lu, and Q. Wang, Theoretical & Applied Mechanics Letters **1**, 033002 (2011).
21. Y. H. Meng, Y. D. Zhang, and J. H. Dai, Science China Technological Sciences **54**, 758 (2011).